

Zirconia Needles Synthesized Inside Hexagonal Swollen Liquid Crystals

Eduardo Pena dos Santos,^{†,‡} Celso Valentim Santilli,[‡]
Sandra Helena Pulcinelli,[‡] and Eric Prouzet^{*,†}

*Institut Européen des Membranes (CNRS UMR 5635), CNRS, 1919 Route de Mende,
F-34293, Montpellier Cedex 5, France, and Instituto de Química, UNESP,
Rua Professor Francisco Degni, s/n CEP 14800-900 Araraquara-SP, Brazil*

Received March 12, 2004. Revised Manuscript Received July 8, 2004

We report the synthesis of zirconia microneedles by the direct nucleation of particles inside a hexagonal swollen liquid crystal (SLC) (cell parameter $a = 27$ nm) prepared by mixing with the proper ratio, an aqueous solution of sulfated zirconium colloids, a cationic surfactant (cetylpyridinium chloride), cyclohexane as swelling agent with an oil over water ratio of 2.5 (vol.), and 1-pentanol as cosurfactant. After a slow crystallogensis that can be enhanced by an initial induction step under moderate temperature, particles in the centimeter range can be obtained, with a very high shape ratio (over 100). These particles are made of crystalline octahydrate zirconium oxychloride containing pores of 20 nm diameter, aligned along the main axis of the liquid crystal, as the fingerprint of the oil cylinders present in the hexagonal phase. The morphology of these particles confirms that the shaping mechanism is based on true liquid crystal templating (TLCT). Further thermal treatment of these particles, after extraction from the SLC, leads to the crystallization of zirconia with the same needlelike morphology as the zirconium oxychloride.

Introduction

Besides its tremendous properties as a thermo-mechanical material or oxygen sensor, stabilized zirconia is currently also studied for more specific applications such as high-temperature NO_x sensor.^{1–9} In these domains, increasing the exchange surface would help to increase the catalytic properties or the sensor efficiency. Different ways were explored to increase the porosity, among them acid-leaching from composite cermet,¹⁰ sol–gel processes,¹¹ addition of organic additives,¹² deposition into the inner pores of mesoporous

MCM-41 silica,⁹ surfactants-based templated structures,^{11–18} or syntheses in microemulsions.^{19,20} In parallel, there is also continuous progress to decrease the size of sensors, to insert them in smaller and smaller systems. This implies that the usual ways to produce materials designed with specific shapes, ceramic processes involving sintering of preshaped powder, may block onto the smaller size threshold and that direct synthesis of predesigned materials should be carried out. Such examples of nanocrystals, fibers, nanorods, or nanowires were reported by various and different processes.^{21–25} We report hereinafter the preparation of macroscopic zirconia particles that exhibit dimensions in the micrometric range along two directions. These

* To whom correspondence should be addressed. E-mail: prouzet@iemm.univ-montp2.fr.

[†] Institut Européen des Membranes, CNRS.

[‡] Instituto de Química, UNESP.

(1) Zhuiykov, S.; Ono, T.; Yamazoe, N.; Miura, N. *Solid State Ionics* **2002**, 152–153, 801.

(2) Szabo, N. F.; Du, H.; Akbar, S. A.; Soliman, A.; Dutta, P. K. *Sens. Actuators, B* **2002**, 82, 142.

(3) Miura, N.; Zhuiykov, S.; Ono, T.; Hasei, M.; Yamazoe, N. *Sens. Actuators, B* **2002**, 83, 222.

(4) Miura, N.; Nakatou, M.; Zhuiykov, S. *Sens. Actuators, B* **2003**, 93, 221.

(5) Nakamura, T.; Sakamoto, Y.; Saji, K.; Sakata, J. *Sens. Actuators, B* **2003**, 93, 214.

(6) Smith, M. R.; Clarke, J. K. A.; Fitzsimons, G.; Rooney, J. J. *Appl. Catal. A* **1997**, 163, 357.

(7) Moran-Pineda, M.; Castillo, S.; Lopez, T.; Gomez, R.; Cordero-Borboa, R.; Novaro, O. *Appl. Catal., B* **1999**, 21, 79.

(8) Labalme, V.; Béguin, B.; Gaillard, F.; Primet, M. *Appl. Catal., A* **2000**, 192, 307.

(9) Sun, Y.; Zhu, L.; Lu, H.; Wang, R.; Lin, S.; Jiang, D.; Xiao, F.-S. *Appl. Catal., A* **2002**, 237, 21.

(10) Kim, H.; da Rosa, C.; Boaro, M.; Vohs, J. A.; Gorte, R. J. *J. Am. Ceram. Soc.* **2002**, 85, 1473.

(11) Takenaka, S.; Takahashi, R.; Sato, S.; Sodesawa, T.; Uematsu, T. *J. Ceram. Soc. Jpn.* **2003**, 111, 16.

(12) Boaro, M.; Vohs, J. A.; Gorte, R. J. *J. Am. Ceram. Soc.* **2003**, 86, 395.

(13) Huang, Y.-Y.; McCarthy, T. J.; Sachtler, W. M. H. *Appl. Catal., A* **1996**, 148, 135.

(14) Suh, Y.-W.; Lee, J.-W.; Rhee, H.-K. *Solid State Sci.* **2003**, 5, 995.

(15) Sun, Y.; Yuan, L.; Wang, W.; Chen, C.-L.; Xiao, F.-S. *Catal. Lett.* **2003**, 87, 57.

(16) Mamak, M.; Métraux, G. S.; Petrov, S.; Coombs, N.; Ozin, G. A. *J. Am. Chem. Soc.* **2003**, 125, 5161.

(17) Yuan, Z. Y.; Vantomme, A.; Léonard, A.; Su, B.-L. *J. Chem. Soc., Chem. Commun.* **2003**, 1558.

(18) Chen, H.-R.; Shi, J.-L.; Li, Y.-S.; Yan, J.-N.; Hua, Z.-L.; Chen, H.-G.; Yan, D.-S. *Adv. Mater.* **2003**, 15, 1078.

(19) Tai, C. Y.; Lee, M.-H.; Wu, Y.-C. *Chem. Eng. Sci.* **2001**, 56, 2389.

(20) Althues, H.; Kaskel, S. *Langmuir* **2002**, 18, 7428.

(21) Chakrabarty, P. K.; Chatterjee, M.; Naskar, M. K.; Siladitya, B.; Ganguli, D. *J. Eur. Ceram. Soc.* **2001**, 21, 355.

(22) Pullar, R. C.; Taylor, M. D.; Bhattacharya, A. K. *J. Eur. Ceram. Soc.* **2001**, 21, 19.

(23) Xu, H.; Qin, D.-H.; Yang, Z.; Li, H.-L. *Mater. Chem. Phys.* **2003**, 80, 524.

(24) Liu, Y.; Zheng, C.; Wang, W.; Zhan, Y.; Wang, G. H. *J. Am. Ceram. Soc.* **2002**, 85, 3120.

(25) Joo, J.; Yu, T.; Kim, W. Y.; Park, H. M.; Wu, F.; Zhang, J. Z.; Hyeon, T. *J. Am. Chem. Soc.* **2003**, 125, 6553.

microneedles of zirconia exhibit a very high shape factor because their length can reach several centimeters. They represent a first step in the future preparation of oxygen microprobes made with Y-doped-zirconia. The present work describes the synthesis process based on shaping by the help of a hexagonal swollen liquid crystal (SLC) made with a quaternary system (oil:water:surfactant:cosurfactant).

This process is relevant of a more general domain, basically the preparation of nanostructured materials with the help of soft matter properties. It may result from two main approaches, one based on assembly forces, for example between micelles and reagents, the other based on confinement inside miniemulsions, microemulsions, or crystallized mesophases. The latter approach using mesophases has been successfully explored.^{26–36} However, from our knowledge, the syntheses in liquid crystals involved only binary (water:surfactant) systems. Quaternary systems (oil:water:surfactant:cosurfactant) may afford new opportunities, but they are expected to be unstable and unable to stand addition of reagents or reactions inside. Oil in water (o/w) miniemulsions obtained after energetic stirring were used for the synthesis of nanoparticles.³⁷ The SLCs used in this study are based roughly on the same components as miniemulsions, but they build hexagonal liquid crystals with infinite cylinders swollen by oil in an aqueous continuous phase, when they are mixed in proper proportions.³⁸ Such a mesophase with nonpolar tubes in a polar medium is defined as a direct phase. Unlike binary liquid crystals, the SLCs contain two phases (oil and water) that can be modified according to the respective proportions of each. Swelling of these hexagonal phases is directed by the increase of the cylinders radius by increasing the amount of oil without changing drastically the distance between them.³⁸ The stability of the hexagonal SLC is also controlled by the correct adjustment of the spontaneous radius of curvature of the surfactant monolayer that builds the cylinder walls. This curvature can adapt to the increasing amount of swelling agent if the ionic force of the aqueous phase is adapted to partially screen the repulsion between charges on the surfactant heads. Therefore, the correct adjustment between the nonpolar solvent swelling the cylinders and salt added in the aqueous phase is a prerequisite factor if one expects these lyotropic systems to display at room temperature a o/w hexagonal phase with amounts of oil that can be twice that of water. The cosurfactant that combines with the surfactant is another factor that helps to stabilize the cylinder

walls. These SLCs offer a large range of possibilities in structure because it has been demonstrated that the correct adjustment between oil and the ionic force of the aqueous solution by addition of a salt allowed the diameter of the nonpolar cylinders to be tuned over 1 order of magnitude (from 3 to 30 nm), while the distance between adjacent cylinders is kept small and nearly constant (about 3 nm).³⁸

In parallel with reactions performed in w/o microemulsions or o/w miniemulsions, these mesophases open a new field of research in the domain of syntheses in liquid crystal because reactions can be performed in the aqueous continuous network or in the oil confined inside cylinders as well as potentially in both together. Unlike previous syntheses in binary liquid crystal, these SLCs are a complex mixture with at least four basic components. Unlike previous reactions performed in miniemulsions, these SLCs are crystallized mesophases that exhibit a long-range order. Their use as nanoreactors is demonstrated in the following by the synthesis of zirconia needles in the aqueous network. The precursors put in the aqueous phase play also the function of the structure-stabilizing salt. Because their concentration is defined by the mesophase geometry, it could be too low to allow the further solid framework from reaching the percolation edge required to build significant particles. A way to overcome this limit is to use colloids instead of salts: a higher amount of matter is then added into the aqueous phase with only a rather slight modification of the ionic force. We report hereinafter a complete description of the synthesis of centrimetric needlelike porous zirconia particles from zirconium sulfate colloids, obtained by combining the destabilization of these colloids by anion exchange with the use of SLCs as structure-directing systems. The shape of the particles synthesized inside the SLC confirms that this mesophase exerts a strong LCT effect on the material shape.

Experimental Section

Synthesis. In the course of preparation of high surface zirconia, a new process involving the pristine formation of sulfated zirconia colloids had been obtained by Chiavacci et al.³⁹ We used the same process for making these colloids, but with higher concentrations than previously reported. These colloids are made of 0.6 nm complexes of zirconium sulfate whose local structure is close to that of $\text{Zr}_{18}\text{O}_4(\text{OH})_{38.8}(\text{OSO}_3)_{12.6}$. They can aggregate to form small clusters with a correlation distance of 3.0 nm, which will give a porous gel after aging.^{39,40} These zirconium sulfate colloids (ZSC) constitute also secondary building blocks that can help to build nanostructured compounds. The synthesis of the ZSC was performed according to previous literature, but with higher concentration ratios. In a typical synthesis, zirconia oxychloride was first dissolved in deionized water to obtain a final solution volume of 500 mL with concentration of 1.5 mol L^{-1} in zirconium. The colloidal suspension was prepared by adding dropwise 450 mL of this aqueous solution into 30 mL of a sulfuric acid solution (1.5 mol L^{-1}) heated at 80°C , under magnetic stirring. One obtained a final $(\text{Zr}^{4+}:\text{H}_2\text{SO}_4)$ molar ratio of 15:1. After cooling, aliquots of 15 mL of the colloidal suspension were put inside an acetyl-cellulose membrane tubing (12–14 000 MW) and then submitted to static dialysis for 24 h against 150 mL of

(26) Ciferri, A. *Prog. Polym. Sci.* **1995**, *20*, 1081.

(27) Attard, G. S.; Glyde, J. C.; Göltner, C. G. *Nature* **1995**, *378*, 366.

(28) Attard, G. S.; Bartlett, P. N.; Coleman, N. R. B.; Elliott, J. M.; Owen, J. R.; Wang, J. H. *Science* **1997**, *278*, 838.

(29) Gabriel, T.; Nandhakumar, I. S.; Attard, G. S. *Electrochem. Commun.* **2002**, *4*, 610.

(30) Göltner, C. G.; Antonietti, M. *Adv. Mater.* **1997**, *9*, 431.

(31) Göltner, C. G.; Berton, B.; Krämer, E.; Antonietti, M. *Adv. Mater.* **1999**, *11*, 395.

(32) Attard, G. S.; Edgar, M.; Göltner, C. G. *Acta Mater.* **1998**, *46*, 751.

(33) Coleman, N. R. B.; Attard, G. S. *Microporous Mesoporous Mater.* **2001**, *44–45*, 73.

(34) Antonietti, M. *Curr. Opin. Colloid Interface Sci.* **2001**, *6*, 244.

(35) Bechinger, C. *Curr. Opin. Colloid Interface Sci.* **2002**, *7*, 204.

(36) El Safty, S. A.; Evans, J. J. *Mater. Chem.* **2002**, *12*, 117.

(37) Antonietti, M.; Landfester, K. *Prog. Polym. Sci.* **2002**, *27*, 689.

(38) Ramos, L.; Fabre, P. *Langmuir* **1997**, *13*, 682.

(39) Chiavacci, L. A.; Santilli, C. V.; Pulcinelli, S. H.; Craievich, A. *F. J. Appl. Crystallogr.* **1997**, *30*, 750.

(40) Chiavacci, L. A.; Pulcinelli, S. H.; Santilli, C. V.; Briois, V. *Chem. Mater.* **1998**, *10*, 986.

deionized water. The concentration of the colloidal suspension was further increased by evaporation at 45 °C under dynamic vacuum up to a final zirconium concentration of 3.4 mol L⁻¹. This is the preparation that is named "sulfate zirconium colloids" (SZC) in the following.

The preparation of the swollen liquid crystal was inspired from that reported by Ramos et al. with anionic sodium dodecyl sulfate, but we chose a cationic surfactant for our synthesis because anionic surfactants lose their surfactant behavior in aqueous solution with a pH below 1.³⁸ The liquid crystal doped with SZC was prepared by the following procedure: 1.0 g of *N*-cetylpyridinium chloride (Acros) was dissolved in 2.0 mL of SZC. This solution could be submitted to a crystallization induction step at temperature up to 56 °C for different times varying from 0 to 8 h. Among all preparations, we describe the results obtained with two samples: sample **A** was not exposed to the induction step and remained at room temperature during the whole process, whereas sample **B** was exposed at 45 °C for 8 h or 56 °C for 4 h. The induction step does not modify the chemical composition or structure of the particles, but it increased the crystallization kinetics and the amount of particles at the expense of the particle size. After cooling, 5 mL of cyclohexane and 300 μ L of 1-pentanol were further added in this solution and mixed vigorously with a vortex shaker, until the formation of a transparent gel formed by the hexagonal liquid crystal. The vessel was sealed and stocked at room temperature for several weeks to let the crystallogenesis proceed: samples **A** and **B** were left for 120 or 60 days, respectively. The SLC was destabilized by the addition of 10 mL of cyclohexane, and the particles were recovered by settling after washing with 20 mL of a mixture of 1-pentanol (1 mL) in cyclohexane (19 mL). This process was repeated three times. We observed that washing with pure pentanol induced the dissolution of crystals, whereas using pure cyclohexane did not allow a perfect separation of crystals from remaining surfactants. Crystals were further dried at room temperature for 72 h, and octahydrated zirconium oxychloride was identified after this step. Calcination (120 °C/6 h, 200 and 600 °C/2 h) led to the formation of zirconia.

Characterization. The structural array of the SLC containing the sulfate zirconium colloids before and after the particle formation was checked by means of small-angle X-ray diffraction (SAXD). SAXD experiments were conducted at the D24 beamline of the DCI synchrotron ring at LURE (Orsay, France). A Ge (111) single-crystal curved monochromator provided a beam focused in the horizontal plane. The selected wavelength was 1.49 Å. The incident beam intensity was monitored by an ionization chamber, and its size (typically 0.4 \times 1.5 mm²) was determined by collimating slits upstream and downstream from the monochromator. To reduce absorption and parasitic scattering, the beam path was kept under vacuum and slits were placed before the sample to suppress the parasitic signal. The sample-to-detector distance was adjusted to 2.50 m to cover the required scattering vector range. The scattering patterns were recorded with an image plate. The samples were placed in a 2.0 mm Lindeman capillary tube. Due to the high intensity, the X-ray diffraction pattern was not corrected for any background scattering. After extraction and drying, the particles were observed by polarized light optical microscopy and scanning electron microscopy (SEM). The optical microscopy was performed with a polarizing Leica DMR optical microscope coupled with a digital camera. The SEM micrographs were obtained on a Hitachi S-5400 FEG microscope, and the samples were fixed on a metallic plate by a graphite tape. A gold thin film was sputtered onto the samples before observation. Crystallization of the particles was studied by means of in situ X-ray powder diffraction (XRPD) with a Philips X-ray PanAnalytical X'pert-Pro (θ - θ) diffractometer coupled with a furnace. The diffractometer is equipped with an Ni filter, X'celerator detector, and Cu K α radiation with a wavelength of 1.5405 Å. The current was adjusted to 40 mA, and the potential was 40 kV. The furnace temperature ramp was adjusted at 20 °C/min and 2 θ step at 0.033°. XRPD patterns were recorded at 25, 200, and 300 °C, and from 5° to 50°, between 400 and 850 °C. TEM observation was performed

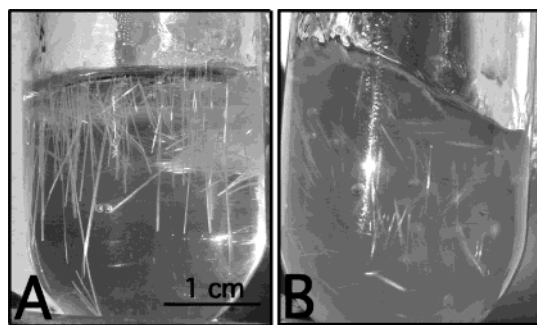


Figure 1. Photos of the reaction vessels of samples **A** and **B**.

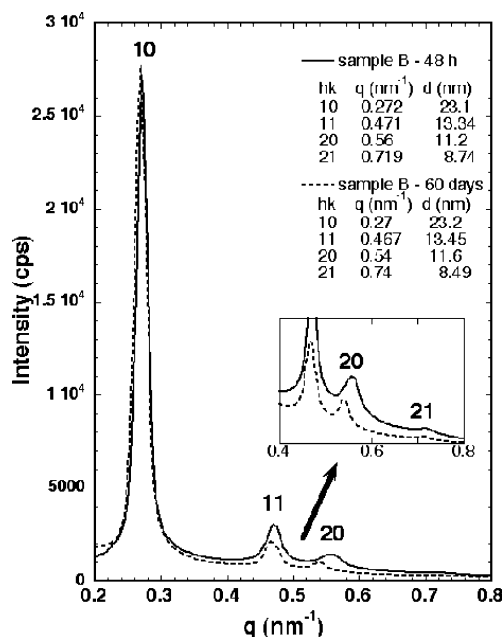


Figure 2. SAXD pattern of SLC containing a zirconium colloidal suspension after 48 h (dark line) and after 60 days (dot line).

with a JEOL JEM 100 CXII transmission electron microscope at an accelerating voltage of 100 kV. The sample drops were deposited and dried on carbon-coated copper grids. Thermogravimetry thermal analysis (TGA) was carried out under air by using a TA TGA2050 high-resolution apparatus. The nitrogen adsorption isotherm was measured at 77 K on a Micromeritics 2010 sorptometer using standard continuous procedures, and samples were first degassed at 150 °C for 15 h. Surface area was determined by the BET method in the 0.05–0.2 relative pressure range.

Results. The crystallogenesis process leads in both cases to the formation of macroscopic needles with a mean shape factor of at least 100 (see Figure 1). One may notice that sample **A** prepared without the induction step presents fewer but bigger particles (crystals length up to 2.0 cm) and their growth occurred mostly from initial seeds at the air/liquid interface. Sample **B** contains more but shorter crystals (crystals length of 0.8 cm), and they are randomly dispersed in the SLC. However, except this difference in size and reaction time, all results further obtained with one sample were similar for the others. We selected hereinafter the results regarding sample **B**, but no difference in the microstructure of thermal evolution was detected between both syntheses.

Figure 2 displays the SAXD pattern obtained on the synchrotron beamline, for sample **B**, after 48 h (before crystallogenesis) and after 60 days (with crystals inside). The presence of four diffraction peaks characteristic of a hexagonal structure (*P6mm*, *a* = 26.6 nm) confirms that the well-ordered structure of the SLC is maintained all over the process and that no change, except a slight increase in the cell parameter,

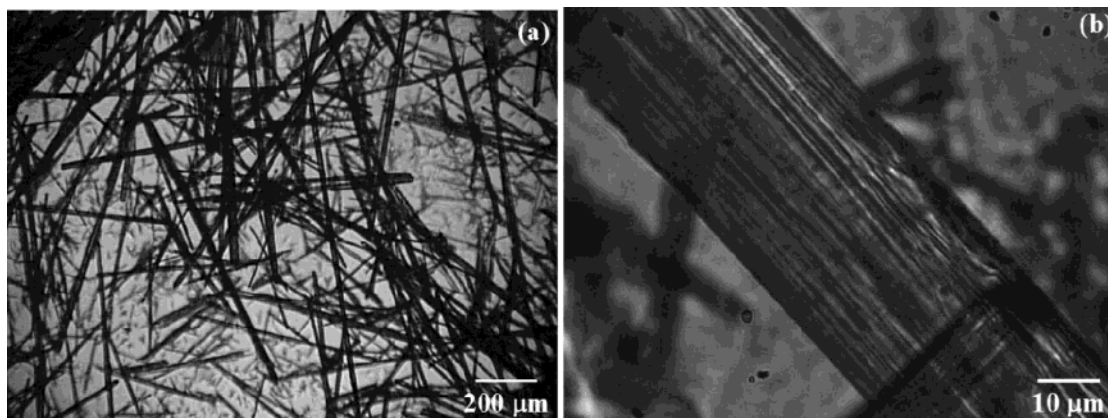


Figure 3. Optical microscopy observation of particles extracted from sample **B**.

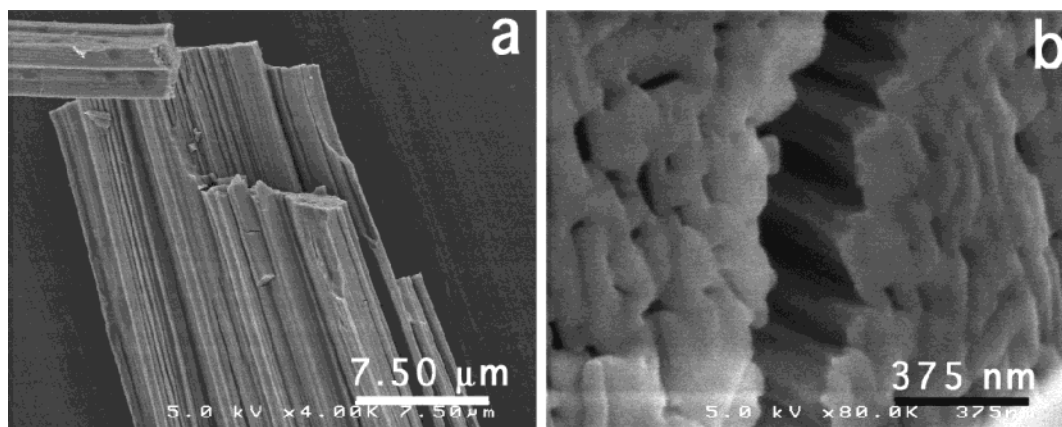


Figure 4. SEM micrographs of crystallized fibers of sample **B**: particle (a) and a close view of a cross section (b).

is observed. These particles were observed after recovery by means of optical microscopy (Figure 3a). All particles observed at this scale present a needlelike structure with length varying from 50 nm to more than 1 cm. The close observation of bigger particles under polarized light reveals a birefringent character (see Figure 3b). Observation by SEM (Figures 4 and SM.1 in Supporting Information) reveals that these needles are actually made of aggregated fibers aligned along the main axis and that this stacking creates interfiber voids whose average diameter can be visually estimated to 20 nm (Figure 4b and SM.1b). The weight losses observed in the TGA curve correspond precisely to those of octahydrated oxychloride zirconium $\text{ZrOCl}_2 \cdot 8\text{H}_2\text{O}$ (Figure SM.2 in Supporting Information). The nature of the material is confirmed by the XRD pattern of raw fibers extracted from the liquid crystal (Figure SM.3 in Supporting Information). Hence, it appears that the crystallization of the sulfate zirconium colloids inside the aqueous framework of the SLC leads first to fibers made of octahydrated zirconium oxychloride.

The structural thermal evolution of the particles was followed by in situ X-ray powder diffraction as a function of the temperature. Figure 5 displays some X-ray patterns of sample **B** selected at different temperatures. Starting at 25 °C with the structure of $\text{ZrOCl}_2 \cdot 8\text{H}_2\text{O}$, a heating at 200 °C induces the dehydration of the sample, giving an amorphous structure up to 350 °C. At 400 °C, the material begins to crystallize as the quadratic ZrO_2 ($P4_2/nmc$), and it evolves progressively toward the monoclinic phase ($P2_1/C$) that begins to be observed at 600 °C. Nevertheless, this evolution from zirconium oxychloride to zirconia through an amorphization step does not alter the general needlelike morphology, as it can be checked by SEM on a sample calcined at 600 °C (Figure 6). Specific surface area and pore size as measured by N_2 adsorption/desorption isotherms show that these particles do not exhibit any significant porosity (specific surface area close to 2 $\text{m}^2 \text{g}^{-1}$). However, a mean pore size calculated with the

4 V/S formula (V , N_2 adsorbed volume; S , specific surface area) can still be estimated at 20 nm, in good correlation with the SEM observation (Figure SM.4 in Supporting Information). A closer analysis of these particles by TEM reveals that they are made of well-organized nanocrystals stacked together along the main axis of the needle (Figure 7).

Discussion

The stability of SLCs is based on a close equilibrium between the quantity of organic swelling solvent (cyclohexane) and the curvature radius of the cylindrical micelle walls made of surfactant (*N*-cetylpyridinium chloride in this case) and cosurfactant (1-pentanol). The charge matching balance in the micelle wall, which allows one to tune the final cylinder curvature, is controlled by the presence of counterions in the aqueous phase, that screen partly the repulsive charge between surfactant heads.³⁸ These counterions are usually brought by a salt such as sodium chloride or sulfate added in the aqueous phase. Instead of a neutral salt, one may choose as SLC stabilizer a precursor of the expected reaction. However, one must bear in mind that the concentration of the precursor is limited by the general geometry of the SLC and that it cannot be fixed independently of it. A too small concentration would prevent any percolation of a continuous framework and would lead at best to single particles. Besides, the advancement of the reaction consumes the precursors, thus the SLC stabilizer, and can lead to its destabilization before the formation of the expected inorganic framework.

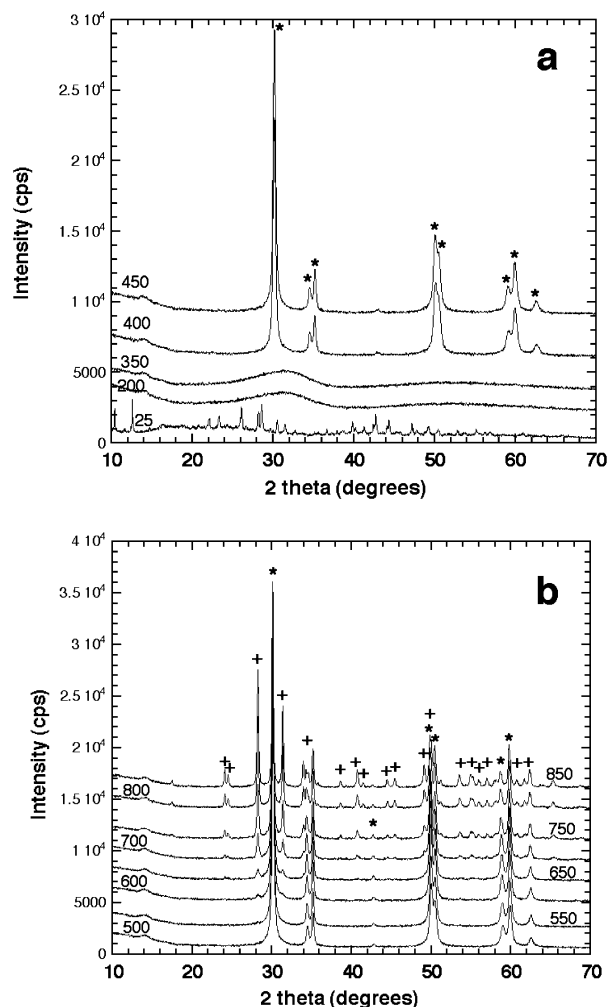


Figure 5. X-ray patterns of sample **B** as a function of the calcination temperature. *, quadratic ZrO_2 (85–1545); +, monoclinic ZrO_2 (78–1807).

For the synthesis of zirconia particles, the reagent itself, that is, the ZCS, substituted the stabilizing salt. As stated before, the use of colloidal particles is a good way to increase the overall concentration in precursors without changing the ionic force of the aqueous phase. Nevertheless, one must point out that the particle size must accommodate the average thickness of the aqueous network: all previous works upon the insertion of colloidal particles reported their insertion into the cylinders of the mesophase, not into the aqueous phase.^{41,42} Another possible drawback of this reaction would be the growth of an isotropic solid if the SLC could not confine it. That would preclude any shape-directing effect of the mesophase. Our study confirms that one can prepare a highly swollen hexagonal mesophase with the sulfate zirconium colloidal solution (Figure 2). Indeed, the mesophase obtained with the SZC and *N*-cetylpyridinium chloride exhibits the same hexagonal structure as those obtained with sodium salts: four peaks are clearly assigned to the hexagonal $P6mm$ group (cell parameter $a = 27$ nm).³⁸ Moreover, the growth of the zirconium oxychloride particles does not impoverish the medium in a way that would modify

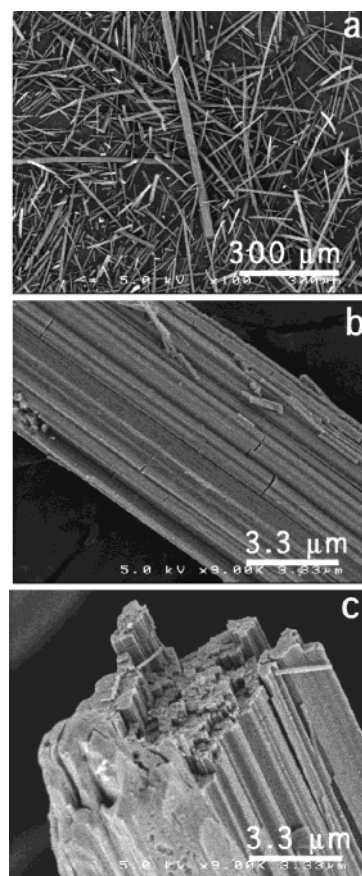


Figure 6. SEM micrographs of ZrO_2 needles extracted from sample **A** and calcined at 600 °C.

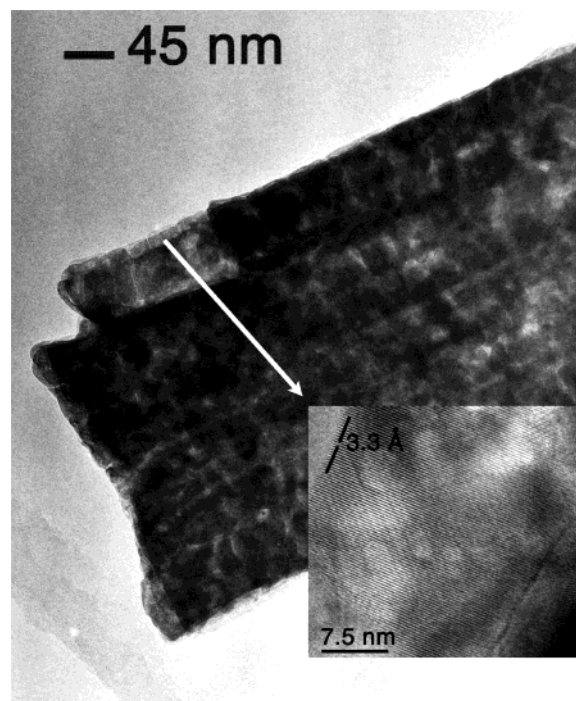


Figure 7. TEM micrograph of ZrO_2 fiber treated at 600 °C.

substantially the ionic force because this sample still exhibits the same structure after 60 days of reaction (Figure 2).

We performed parallel trials to study the possible growth of zirconium oxychloride in bulk water. Surprisingly, when the SZC was let alone at rest for several

(41) Ramos, L.; Fabre, P.; Ober, R. *Eur. Phys. B* **1998**, *1*, 319.

(42) Eiser, E.; Bouchama, F.; Thathagar, M. B.; Rothenberg, G. *ChemPhysChem* **2003**, *4*, 526.

weeks, no reaction occurred and the solution remained perfectly stable. The formation of particles was observed only when the solubility of these colloids was decreased by cooling the solution below 10 °C. In this case, the particles exhibit a lamellar structure that does not correspond to that observed in the SLC (see Figure SM.5 in Supporting Information). A similar trend is also observed when one increases the concentration of the colloidal solution.

In our study, the crystallization in the SLC leads to the pristine formation of octahydrated zirconium oxychloride. The origin of the chloride ions is the counterions of CTPCl. Hence, the first action of the SLC is a chemical effect with the exchange between chloride counterions of CTPCl with the sulfate ions present in the colloidal suspension, which, of course, cannot be observed with the colloidal suspension alone. The further crystallization process itself is based on a classical nucleation and growth mechanism. The nucleation is induced either by a local concentration increase (crystallization of particles at the air–SLC interface for sample **A**) or by the temperature (sample **B** at 56 °C at 4 h) when the mixture of the SZC with the surfactant is left for several hours at moderate temperature before the formation of the liquid crystal. As compared to sample **A**, reactions performed with sample **B** allowed us to obtain numerous but smaller crystals in a shorter reaction time due to the formation of a larger amount of seeds. This was verified with different samples left at different temperatures (45 or 56 °C) for durations between 2 and 8 h.

If the kinetics of crystal formation depends on the occurrence of the induction step, the micrographs of both samples show that the morphology and the lateral dimensions of the crystals do not. The formation of one-dimensional particles must be closely related with the anisotropy of the hexagonal swollen liquid crystal that can form large single domains. Nucleation of zirconium oxychloride is thus confined in the interspace between the cylinders of the organic phase, and it leads to fibers that will further aggregate inside the SLC with the cylinders trapped by the solid framework at the origin of the future pores of 20 nm in diameter, as revealed by SEM (Figures 4.b and SM.1) and confirmed by N₂ isotherm measurements (Figure SM.4). Hence, the final morphology of the needles appears as built from the aggregation of smaller microfibers that grew along the main axis of the hexagonal liquid crystal, fed by the diffusion of colloids in the aqueous phase up to the first

seeds, and further aggregated by trapping the oil cylinders of the liquid crystal (Figure SM.1). The true liquid crystal templating (LCT) mechanism is thus confirmed, and it appears that it extends to dimensions far longer than have been reported until now, because crystals up to 2 cm can be observed.

Finally, the thermal treatment of the needles after recovering from the SLC induces the dehydration of ZrOCl₂·8H₂O that leads to a total amorphization of sample at 200 °C, but without any loss in the particle morphology acquired during the fiber formation. The initial shape is maintained all over the thermal treatment, and the particles obtained at 600 °C and higher exhibit the same needlelike shape. The zirconia needles are made of nanodomains of perfectly crystallized zirconia.

We demonstrate in this report that the swollen liquid crystal (SLC) that had been defined for anionic surfactants can be prepared also by the use of cationic *N*-cetylpyridinium chloride and used as a new nanoreactor. Colloidal suspensions can be added into it and lead to a continuous framework if they are suitably destabilized. In our example, this approach allowed us to produce crystalline ZrOCl₂·8H₂O as well as ZrO₂ needles after thermal treatment. These one-dimensional particles appear to be good candidates for future development as oxygen microprobes, for instance, once yttrium doping will be achieved. This latter step is presently in progress.

Acknowledgment. We thank Dr. Patricia Kooyman from the Delft HRTEM Centre for TEM observations, Claudie Bourgaux and all of the staff from LURE for help in SAXD measurements using the synchrotron source, Arie van der Lee for help with in situ XRD measurements, and Prof. Dr. Antonio Carlos Guastaldi and Márcio Luis dos Santos for their help in optical microscopy. We also thank the French Ministry of Research and Education for its financial support through the “ACI Nanosciences” funding program, and French (COFECUB) and Brazilian (CAPES and FAPESP) organizations for their financial support in the SOL French-Brazilian network. E.P.S. is grateful for Ph.D. funding.

Supporting Information Available: SEM photos and experimental plots (PDF). This material is available free of charge via the Internet at <http://pubs.acs.org>.

CM049589H